creased slightly above 288 K.[2] These results were interpreted in terms of exchange of water molecules between high energy or tight binding sites and secondary sorbtion sites with less binding energy.[2] Our results can be interpreted in a similar manner. At temperatures below 295 K, T_{2b} and T_{2f} are sufficiently different ($T_{2c} \sim 8$–30 μs, $T_{2f} \sim 700$ μs at 295 K)[2] and the rates of exchange between the phases are slow enough to permit the observation of the two phases separately. As the temperature is increased, the rates of exchange between the phases increase rapidly and the distinction between the phases can no longer be made. The T_2 mechanisms now include a contribution from the exchange process which increases with temperature, giving rise to an eventual minimum in T_2 or a plateau region depending on the distribution of barrier heights to exchange.[3] It therefore appears that as the temperature is increased exchange of water molecules between the bound water phase and free water becomes rapid thereby making the distinction between the two impossible. The decrease in T_{2c} at the higher temperatures cannot be explained at this time except to postulate that as the temperature is increased the cellulose structure opens up probably allowing exchange between the tightly bound phase and the newly created sites. The fact that the initial steep rise in T_{2c} observed at lower temperatures is not found for samples above room temperature also tends to suggest that as the structure opens up and the intrinsic processes of the cellulose chains become fairly rapid the primary adsorption process (up to the point of plasticization) does not impart additional motion to the system.

References and Notes

(1) M. F. Froix and R. Nelson, *Macromolecules*, 8, 726 (1975).
(2) T. F. Child, *Polymer*, 13, 259 (1972).
(3) H. A. Resing, *Adv. Mol. Relaxation Processes*, 1, 119 (1968).

Configurational Thermodynamic Properties of Polymer Liquids and Glasses. Poly(vinyl acetate). II

John E. McKinney[1a] and Robert Simha*[1b]

Institute for Materials Research, National Bureau of Standards, Washington, D.C. 20234, and the Department of Macromolecular Science, Case Western Reserve University, Cleveland, Ohio 44106. *Received February 6, 1976*

ABSTRACT: The theoretical internal energy, entropy, and internal pressure of the equilibrium system of poly(vinyl acetate) using the scaling parameters established previously are computed as functions of temperature and pressure and found to be in good agreement with those derived from the experimental PVT data given in paper I. For the analysis of the glassy state, a new method is developed and applied to the two constant formation glasses discussed earlier. It employs the partition function which has the same mathematical form as for the equilibrium system, but derives the hole fraction $h(V, T)$ as the solution of a partial differential equation. This equation results from the proper thermodynamic definition of the pressure in terms of the partition function, applied to the experimental PVT surfaces for the glasses. A quantitative improvement in the compressional thermodynamic functions, particularly in regard to the internal pressure, ensues over the more empirical procedure employed previously. There h is treated as an adjustable parameter in the pressure equation derived for the liquid, using the experimental PVT surface for the glass. The application of the proper expression for the pressure results in a reduced variation of h with temperature and pressure in the glassy state and thus in numerically larger freezing fractions than those derived earlier. We exhibit the internal energy and entropy differences between the atmospheric pressure and pressurized (800 bar) glasses, and between these and the super-cooled melt. The computed difference between the configurational heat capacities of the melt and glass at T_g are about 47% for C_p and 13% for C_v of the totals obtained by calorimetry. Finally, convenient interpolation expressions for the hole fraction, theoretical internal energy, and theoretical entropy as functions of the reduced variables of state are developed for the equilibrium liquid in general and the two specific glasses considered here. These relations dispense with the necessity of iteration procedures for the numerical evaluation of the theoretical functions.

In a recent paper[2] (paper I) we have analyzed the liquid and glassy states of polymers in terms of theory and based on experimental data for poly(vinyl acetate).[3] The discussion was concerned with the PVT (pressure–volume–temperature) relations applicable to the liquid (equilibrium) region and glasses formed by variable and constant formation histories. With the variable formation history the properties of the glass are obtained by isobaric cooling at one constant rate at different pressures always commencing at temperatures sufficiently large to attain initial equilibrium. The intersection of the extrapolated liquid and glass PVT surfaces gives the proper glass transition temperature $T_g(P)$. With the constant formation history the glass is formed by isobaric cooling at one pressure P' (0 or 800 bar) with subsequent measurements in the glass being made at additional pressures. The intersection of the liquid and glass surfaces gives $T_g^{\dagger}(P,P')$. Since all data points of the constant formation glass pertain to one formation pressure P', and since no structural relaxation was observed after glass formation, the corresponding PVT surface is taken to be reversible, yielding proper thermodynamic quantities even though true equilibrium is not attained. For further details, see ref 3. The discussion in paper I encompasses first the liquid equilibrium state, second the liquid–glass transition line and the relationship between the pressure coefficients dT_g/dP and $dT_g^{\dagger}/dP$ of glasses formed under the variable and constant formation histories, respectively, and third the equation of state for the glasses of the latter kind. Of central importance in this analysis is the behavior of the ordering parameter y, the fraction of occupied sites, in the three regions mentioned above.

The purpose of this paper is to present a discussion of the configurational thermodynamic functions, in particular those which can be derived from PVT measurements and compared with theoretical predictions. We have previously shown some

Table I

(a) Coefficients for the Hole Fraction $h(\tilde{T}, \tilde{V}) = \sum_{i=0}^{2} \sum_{j=0}^{2} a_{ij} \tilde{T}^i \tilde{V}^j$

		Glass	
	Liquid[a]	$\tilde{P}' = 0$	$\tilde{P}' = 0.0853$
	$0.025 \leq \tilde{T} \leq 0.040$	$0.025 \leq \tilde{T} \leq 0.031$	$0.025 \leq \tilde{T} \leq$
	$0.96 \leq \tilde{V} \leq 1.10$	$1.00 \leq \tilde{V} \leq 1.03$	$(0.031 + 0.040\,\tilde{P})$
			$0.99 \leq \tilde{V} \leq 1.03$
ij	$(0 \leq \tilde{P} \leq 0.1)$	$(0 \leq \tilde{P} \leq 0.0853)$	$(0 \leq \tilde{P} \leq 0.0853)$
00	0.054492	-0.0011	0.0674
01	0.49570	0.0240	-0.035
02	0.6099		
10	2.2824		-2.99
11	1.374	2.75	4.45
12	-65.41		
20	-25.59	-36.5	-12.6
21	93.2		
22	1718		
SD Δh	0.72×10^{-5}	0.74×10^{-4}	0.94×10^{-4}

(b) Coefficients for the Hole Fraction $h(\tilde{T}, \tilde{P}) = \sum_{i=0}^{2} \sum_{j=0}^{2} a_{ij} \tilde{T}^i \tilde{P}^j$

		Glass			
		$\tilde{P}' = 0$		$\tilde{P}' = 0.0853$ (800 bar)	
	Liquid	$0.025 \leq \tilde{T} \leq 0.031$		$0.025 \leq \tilde{T} \leq (0.031 + 0.040\tilde{P})$	
	$0.025 \leq \tilde{T} \leq 0.040$	$0 \leq \tilde{P} \leq 0.0853$		$0 \leq \tilde{P} \leq 0.0853$	
ij	$0 \leq \tilde{P} \leq 0.100$	A.P.	P.F.	A.P.	P.F.
00	-0.08350	0.03074	0.04452	0.02391	0.03470
01	0.0724	0.0215		0.0159	0.0183
02					
10	4.316	1.457	1.036	1.420	1.071
11	-5.93	-2.26	-0.889	-1.87	-1.41
12					
20	21.42				
21	-121.6				
22	465.4				
SD Δh	0.76×10^{-4}	1.1×10^{-4}	1.0×10^{-4}	1.3×10^{-4}	1.0×10^{-4}

[a] For liquid coefficients, the variables $\tilde{T}$ and $\tilde{V}$ are replaced by $\tilde{T} - 0.03$ and $\tilde{V} - 1$.

examples of compressional energy changes for styrene[4a] and methacrylate[4b,5] derivatives in the liquid state, noted the good agreement between experiment and theory, and commented on the deviations in respect to the internal pressures, which although quantitatively moderate, are significant. Here we consider the glassy state as well, and examine the consistency of the assumptions made in formulating an equation of state using the experimental thermodynamic functions. It will be recalled from paper I that the hole fraction h in the glass was treated as a disposable parameter, with a pressure and temperature dependence below T_g derived from the experimental equation of state.[2,4-6] As demonstrated here and in paper I, the significance of these efforts lies first in testing the equilibrium theory of the liquid state, and second in extending the tests of the assumptions made in respect to the glassy state, specifically testing the gradual freeze-in of the ordering parameter h below T_g and comparing the results for different formation conditions. This will give us confidence in the results of the computations presented later in this paper on the configurational contributions to the enthalpy and entropy at atmospheric pressure and corresponding heat capacities, which are not readily accessible experimentally. A calculation of the differences between certain thermodynamic functions for the supercooled liquid and the corresponding states in the glass is important in connection with kinetic studies as well.

As with order parameter theory in general, our approach excludes the free energy of the glass from reaching a local minimum with respect to the ordering parameter h. We do not, however, have a theoretical constraint condition for the glass. The constraints on h are such that its temperature and pressure dependences are determined numerically from experimental values of volume at different temperatures and pressures.

Treatment of Experimental Data

We continue with the use of the Tait equation to represent the PVT observations, viz.:

$$1 - V/V_0 = 0.0894 \ln [1 + (P - P_0)/B(T)] \quad (1)$$

with $B(T) = a \exp(-bT)$, where V_0 is the volume V at pressure $P = P_0$ for which in this work $P_0 = 0$. The temperature dependent values of V_0 and of the coefficients a and b for the liquid and three different glasses have been given in ref 2, Tables I and II. The explicit dependence of the internal pressure P_i on the independent variables is obtained by substitution of eq 1 into the definition

$$P_i = (\partial U/\partial V)_T = T(\partial P/\partial T)_V - P \quad (2)$$

Table II

(a) Coefficients for $\tilde{U}(\tilde{T}, \tilde{V})$: $\tilde{U}(\tilde{T}, \tilde{V})^a = \sum_{i=0}^{2} \sum_{j=0}^{2} a_{ij} \tilde{T}'^i \tilde{V}'^j$

		Glass	
	Liquid	$\tilde{P} = 0$	$\tilde{P}' = 0.0853$
	$0.025 \leq \tilde{T} \leq 0.040$	$0.025 \leq \tilde{T} \leq 0.031$	$0.025 \leq \tilde{T} \leq (0.030 + 0.040\tilde{P})$
	$0.96 \leq \tilde{V} \leq 1.10$	$1.00 \leq \tilde{V} \leq 1.03$	$0.99 \leq \tilde{V} \leq 1.03$
	$(0 \leq \tilde{P} \leq 0.1)$	$(0 \leq \tilde{P} \leq 0.0853)$	$(0 \leq \tilde{P} \leq 0.0853)$
ij			
00	-0.67587	-0.66750	-0.67176
01	0.42853	0.2003	0.2238
02	0.5962	1.245	1.727
10	1.2532	0.8935	0.6699
11	-3.382		
12	-48.4	-258	
20	-4.01	5.74	
21	116.4		-322
22	1156		
SD $\Delta\tilde{U}$	0.14×10^{-4}	0.29×10^{-4}	0.38×10^{-4}

(b) Coefficients for $\tilde{U}(\tilde{T}, \tilde{P})$ and $\tilde{S}(\tilde{T}, \tilde{P}) - \ln V^* - \text{const}$: $f(\tilde{T}, \tilde{P}) = \sum_{i=0}^{2} \sum_{j=0}^{2} a_{ij} \tilde{T}^i \tilde{P}^j$

			Glass			
	Liquid		$\tilde{P}' = 0$		$\tilde{P}' = 0.0853$	
	$0.025 \leq \tilde{T} \leq 0.040$		$0.025 \leq \tilde{T} \leq 0.031$		$0.025 \leq \tilde{T} \leq (0.030 + 0.040P)$	
	$0 \leq \tilde{P} \leq 0.100$		$0 \leq \tilde{P} \leq 0.0853$		$0 \leq \tilde{P} \leq 0.0853$	
ij	$\tilde{U}$	$\tilde{S} - C^b$	$\tilde{U}$	$\tilde{S} - C^b$	$\tilde{U}$	$\tilde{S} - C^b$
00	-0.77436	-10.5100	-0.720 89	-7.810	-0.673 51	-5.899
01		-2.60	1.184	30.88	-1.002	-42.76
02	0.308	3.42	-10.73	-305.0	9.23	372
10	3.14	225.93	2.610	147.8	-1.135	
11	-2.68	-123.5	-90.45	-2500	69.87	2893
12	-16.6		803.7	22810	-648.0	-26300
20	15.14	-1504.5	-19.9	-1680	46.6	940.2
21	-118.4		1620	46300	-1309	-52100
22	625	4750	-14760	-422000	11540	465000
SD Δf	0.53×10^{-4}	0.11×10^{-2}	0.41×10^{-4}	0.12×10^{-2}	0.53×10^{-4}	0.17×10^{-2}

$^a \tilde{T}' = \tilde{T} - 0.03$, $\tilde{V}' = \tilde{V} - 1$. $^b C = \ln V^* + \text{const}$.

where U is the internal energy. Accordingly, from eq 1,

$$P_i = (T\alpha_0/0.0894)(P + B)[1 - 0.0894 \ln (1 + P/B)] + P(\mathrm{d} \ln B/\mathrm{d} \ln T - 1) \quad (3)$$

where $\alpha_0 = (1/V_0)(\partial V/\partial T)_{P=0}$. The internal energy difference

$$\Delta U = U(V,T) - U(V_0,T) = -(T\alpha_0/0.0894 + T\,\mathrm{d} \ln B/\mathrm{d}T + T\alpha_0 - 1)0.0894PV_0 + 0.0894V_0[T\alpha_0(P + B) + B(\mathrm{d} \ln B/\mathrm{d} \ln T - 1)] \ln (1 + P/B) \quad (4)$$

is obtained by integration of eq 2 with respect to V at constant T. Finally, we have for the corresponding entropy difference ΔS,

$$T\Delta S = \Delta U + \int_{V_0}^{V} P\,\mathrm{d}V = \Delta U + B(V_0 - V) - 0.0894V_0P \quad (5)$$

Numerical results for the liquid and the two glasses formed at atmospheric and 800 bar pressure respectively will be displayed below. Note that the energy $U(V,T)$ and hence $U(V_0,T)$ cannot be evaluated from PVT data solely. $U(V_0,T)$ may be obtained by integration of the heat capacity C_p between absolute zero and T. The analogous argument applies to the entropy.

Theoretical Formulation

The formulation given previously[2,7] is reviewed and extended to include nonequilibrium glassy behavior and additional thermodynamic functions. For a single ordering parameter, which here is the fraction of occupied sites y, we make use of the thermodynamic definitions

$$-P = -P_1 - P_2 = (\partial F/\partial V)_{T,y} + (\partial F/\partial y)_{V,T}(\partial y/\partial V)_T \quad (6)$$

$$-S = -S_1 - S_2 = (\partial F/\partial T)_{V,y} + (\partial F/\partial y)_{V,T}(\partial y/\partial T)_V \quad (7)$$

where $F = -kT \ln Z$ is the Hemholtz free energy determined from the configurational partition function $Z(\tilde{V},\tilde{T},y)$ given in ref 7. The universal reduced variables $\tilde{X}_i$ (for example, $\tilde{P}$, $\tilde{V}$, and $\tilde{T}$) are related to the corresponding experimental ones X_i through $\tilde{X}_i = X_i/X_i^*$, where X_i^* are the scaling factors taken as constants for each substance. Although the values of the scaling factors are normally determined through superposition of PVT data, as demonstrated in paper I, they also are defined explicitly in terms of molecular parameters.

The explicit dependences of the above free energy derivatives in terms of the theoretical reduced variables are

$$(\partial\tilde{F}/\partial y)_{\tilde{T},\tilde{V}} = -(3\tilde{T}/y)(s/3c)[1 + \ln (1 - y)/y] + (3\tilde{T}/y)[2^{-1/6}y(y\tilde{V})^{-1/3} - \tfrac{1}{3}][1 - 2^{-1/6}y(y\tilde{V})^{-1/3}]^{-1} + \tfrac{1}{2}(yV)^{-2}[2.409 - 3.033(y\tilde{V})^{-2}] \quad (8)$$

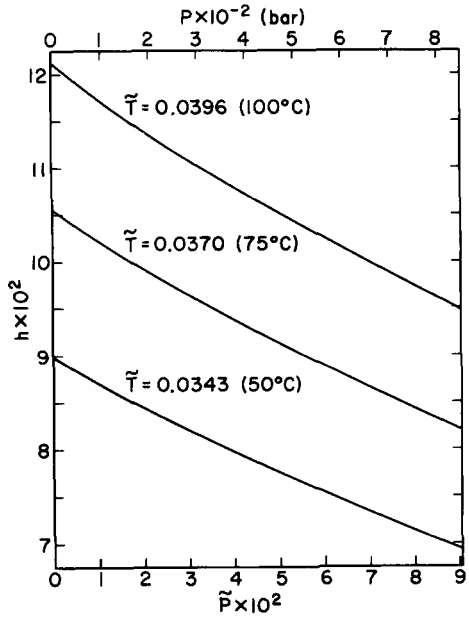

Figure 1. Equilibrium hole fraction h as a function of pressure at three temperatures.

$$(\partial\tilde{F}/\partial\tilde{V})_{\tilde{T},y} = -(\tilde{T}/\tilde{V})[1 - 2^{-1/6}y(y\tilde{V})^{-1/3}]^{-1} - (2y/\tilde{V})(y\tilde{V})^{-2}[1.011(y\tilde{V})^{-2} - 1.2045] \quad (9)$$

and,

$$(\partial\tilde{F}/\partial\tilde{T})_{\tilde{V},y} = (1/c)\ln y + (s/c)[(1-y)/y]\ln(1-y) - 3\ln[(y\tilde{V})^{1/3} - 2^{-1/6}y] - \ln V^* + \text{const} \quad (10)$$

where the constant term involves a positive quantity which cannot be determined from the PVT data. s and $3c$ are the number of segments per chain and the number of external degrees of freedom per chain, respectively. The ratio $s/3c$ will be taken to be unity here as in previous work.

At equilibrium the second terms on the right-hand side of eq 6 and 7 vanish by virtue of the minimization condition $(\partial F/\partial y)_{T,V} = 0$. Accordingly, any general thermodynamic function may be expressed as a sum of two terms as indicated: one which has the same form as the function at equilibrium (subscript 1), and one which includes the additional terms (subscript 2). From eq 6 and the minimization condition, we obtain at equilibrium:

$$\tilde{P}\tilde{V}/\tilde{T} = [1 - 2^{-1/6}y(y\tilde{V})^{-1/3}]^{-1} + (2y/\tilde{T})(y\tilde{V})^{-2}[1.011(y\tilde{V})^{-2} - 1.2045] \quad (11)$$

and

$$(s/3c)[(s-1)/s + y^{-1}\ln(1-y)] = (y/6T)(y\tilde{V})^{-2}[2.409 - 3.033(y\tilde{V})^{-2}] + [2^{-1/6}y(y\tilde{V})^{-1/3} - \tfrac{1}{3}][1 - 2^{-1/6}y(y\tilde{V})^{-1/3}]^{-1} \quad (12)$$

where the term $(s-1)/s$ approaches unity for long chains. From the simultaneous solution of these two equations we determine $y(\tilde{T},\tilde{V})$ and the pressure numerically. Knowing y, we derive the equilibrium configurational entropy from the equation

$$\tilde{S} = \tilde{S}_1 = -(1/c)\ln y - (s/c)[(1-y)/y]\ln(1-y) + 3\ln[(y\tilde{V})^{1/3} - 2^{-1/6}y] + \ln V^* + \text{const} \quad (13)$$

which is obtained from eq 7. Note that the first term is negligible for long chains as in eq 10.

From the relation

$$U = F + TS = F - T(\partial F/\partial T)_{V,y} - T(\partial F/\partial y)_{V,T}(\partial y/\partial T)_V \quad (14)$$

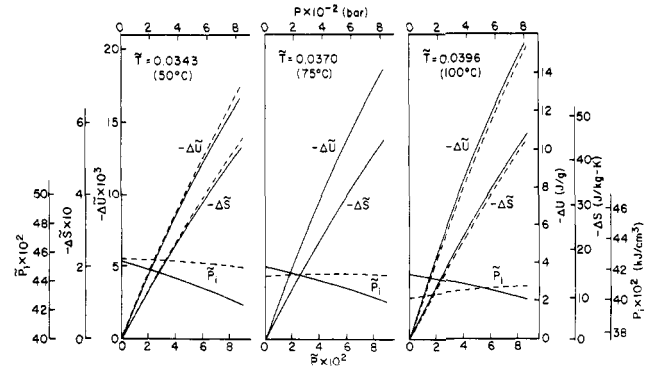

Figure 2. Internal energy and entropy changes and internal pressure as a function of pressure at three temperatures. Dashed lines, experimental, eq 4, 5, 3; solid lines, theoretical, eq 15, 13, 17.

it is apparent that U may also be written in the form $U = U_1 + U_2$ with $U = U_1$ at equilibrium for which the corresponding reduced variable is

$$\tilde{U}_1 = (y/2)(y\tilde{V})^{-2}[1.011(y\tilde{V})^{-2} - 2.409] \quad (15)$$

and, as apparent from eq 7 and 14, $U_2 = TS_2$.

The internal pressure

$$P_i = (\partial U/\partial V)_T = T(\partial P/\partial T)_V - P \quad (16)$$

at equilibrium in terms of the reduced variables is

$$\tilde{P}_i = (2y/\tilde{V})(y\tilde{V})^{-2}[1.2045 - 1.011(y\tilde{V})^{-2}] + (y\tilde{V})^{-2}[1.2045 - 1.5165(y\tilde{V})^{-2}](\partial y/\partial\tilde{V})_{\tilde{T}} \quad (17)$$

where

$$(\partial y/\partial\tilde{V})_{\tilde{T}} = (y/\tilde{V})\{\tfrac{2}{3}[1 - 2^{-1/6}y(y\tilde{V})^{-1/3}]^{-2}2^{-1/6}y(y\tilde{V})^{-1/3} - (y/2\tilde{T})(y\tilde{V})^{-2}[12.132(y\tilde{V})^{-2} - 4.818]\} \times \{\tfrac{4}{3}[1 - 2^{-1/6}y(y\tilde{V})^{-1/3}]^{-2}2^{-1/6}y(y\tilde{V})^{-1/3} + (y/2\tilde{T})(y\tilde{V})^{-2}[9.099(y\tilde{V})^{-2} - 2.409] + 3[y^{-1}\ln(1-y) + (1-y)^{-1}]\}^{-1} \quad (18)$$

is obtained by differentiating eq 12.

The theoretical equilibrium differences $\Delta\tilde{U}$ and $\Delta\tilde{S}$ corresponding to the experimental ones [eq 4 and 5] are readily obtained from eq 15 and 13, respectively.

The methods used to determine $(\partial y/\partial V)_T$ and $(\partial y/\partial T)_V$ for the extension of the thermodynamic functions to the glassy state are discussed in the next section.

Evaluation of the Thermodynamic Functions

A. The Liquid State. In ref 2 the scaling factors $T^* = 9419$ K, $P^* = 9380$ bar, and $V^* = 0.8141$ cm³/g were obtained for PVAc. In what follows we will make use of the additional scaling parameters for the internal energy $U^* = P^*V^* = 763.6$ J/g, and $S^* = P^*V^*/T^* = 81.07$ J/(kg K) for the entropy.

In Figure 1 isotherms for the hole fraction $h = 1 - y$ at equilibrium are displayed. It will be noted that h is reduced by about the same amount through the application of pressure (~21%/800 bar) over the whole range of temperatures. The results for the pressure dependence of the thermodynamic functions at the temperatures used in Figure 1 are illustrated in Figure 2. The good agreement in respect to the internal energy difference ΔU is in line with our expectations from previous work.[4,5] The numerically small differences (maximally about 4%) change sign with increasing temperature. The entropy difference ΔS follows the same pattern, since the theoretical isotherms are accurate. The deviations in respect to the internal pressure are of the same order of magnitude. However, the theory predicts a significantly larger pressure

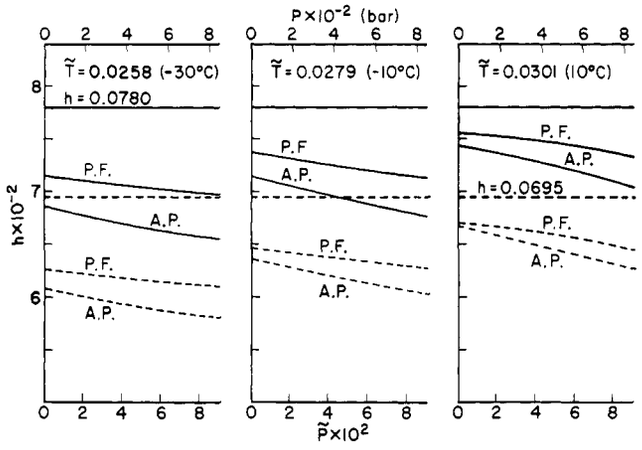

Figure 3. Hole fraction h as a function of pressure at three temperatures. Solid lines, low pressure ($\tilde{P}' = 0$); dashed lines, high pressure glass ($\tilde{P}' = 0.0853$). A.P., adjusted parameter, P.F., partition function procedure. Horizontal line values at T_g.

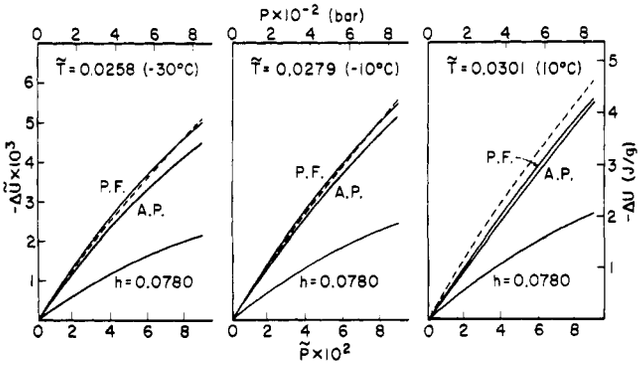

Figure 4. Compressional internal energy as a function of pressure for low pressure glass ($\tilde{P}' = 0$). Dashed lines, experimental (Tait equation); solid lines, A.P., P.F., and frozen parameter assumption (h = 0.0780).

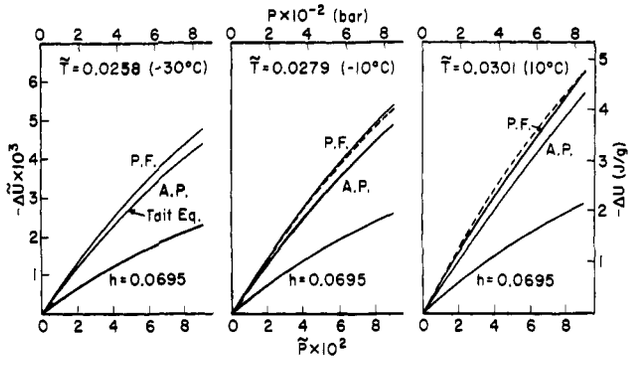

Figure 5. Compressional internal energy as a function of pressure for high pressure glass ($\tilde{P}' = 0.0853$). Dashed lines, experimental (Tait equation); solid lines, A.P., P.F., and frozen parameter assumption (h = 0.0695).

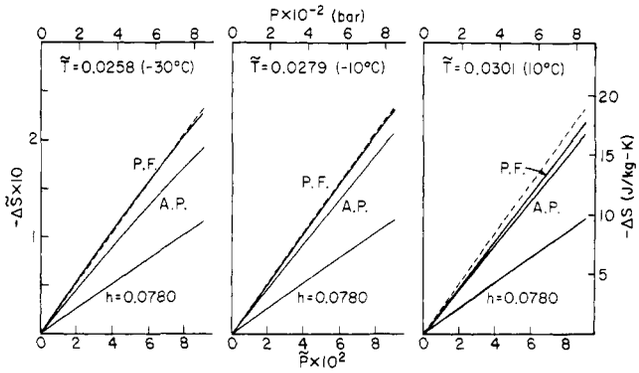

Figure 6. Compressional entropy as a function of pressure for low pressure glass ($\tilde{P}' = 0$). Dashed lines, experimental (Tait equation); solid lines, A.P., P.F., and frozen parameter assumption.

dependence than is observed. The experimental internal pressures exhibit a maximum over the available range. The corresponding maximum for the theoretical internal pressures would occur at negative pressure at these temperatures, or at positive pressures at temperatures well above our experimental range. Now, the internal pressure maximum corresponds to the inflection to the right of the minimum of the potential energy distance curve. It is an open question to what extent this discrepancy reflects the assumed 6–12 intersegmental potential or is inherent in the underlying quasilattice model.[7] In any case, the deviations become pronounced in the third derivatives of the partition function.

B. The Glassy State. The following discussion refers to two systems prepared under different but constant formation pressures (0 to 800 bar) during cooling at a constant rate of 5 °C/h.[3] In paper I we have applied an earlier procedure[6] in which the equilibrium condition, eq 12, is replaced by an empirical adjustment of y to the experimental through the theoretical equation of state, eq 11, where $\tilde{P}$, $\tilde{V}$, and $\tilde{T}$ take on their reduced experimental values. This procedure is not strictly proper, however, because eq 11 is obtained by ignoring the contribution of the right-hand term (P_2) of eq 6. This term vanishes at equilibrium for which $(\partial F/\partial y)_{V,T} = 0$, or if y is constant, neither of which are satisfied in the glass. This kind of analysis has allowed us to characterize structurally different polymer glasses in terms of a freezing fraction[2,5,8] which is a measure of the variation of the hole fraction with temperature or pressure in the glass relative to that in the liquid state. We can now continue to employ this empirical function and compute thermodynamic functions by means of eq 13, 15, and 17. Since neither of the two conditions above are satisfied in the glass, this procedure, of course, cannot be justified on a consistent statistical mechanical basis, even after accepting the above procedure in connection with the equation of state. Recalling however the basic model of a quasilattice underlying the development of the theory,[7] the expression for $\tilde{U}$, eq 15, may be regarded simply as a lattice sum. The accuracy of U so computed with the aid of the dependence of y on $\tilde{V}$ and $\tilde{T}$, then determines that of ΔS, calculated from eq 13, which is tantamount to that obtained by evaluating the integral $\int P\,dV$ [see eq 5]. In Figure 3 the lines marked by A.P. (adjustable parameter) show the requisite isotherms of h. The results for the two glasses which are derived from eq 11 once more indicate the significant departures from the values at the glass temperature marked by the horizontal lines.

The consequence of these computations for the energy is illustrated in Figures 4 and 5 by the curves marked as A.P. Also exhibited are the ΔU's derived from eq 15 by assuming a complete freeze-in (constant h), where h assumes its value at $T_g(P')$. As anticipated, the resulting deviations from the experimental functions are pronounced in this case and similar to those noted for poly(cyclohexyl methacrylate).[5] The results are encouraging in that an empirical adjustment of the theoretical equation of state yields a quite satisfactory estimate of the compressional energy difference and hence also the entropy difference. We note however increasing deviations with increasing pressure in Figures 4 and 5 for the curves labeled A.P. No distinction in this respect between the low and high pressure formation glass is evident. The entropy lines

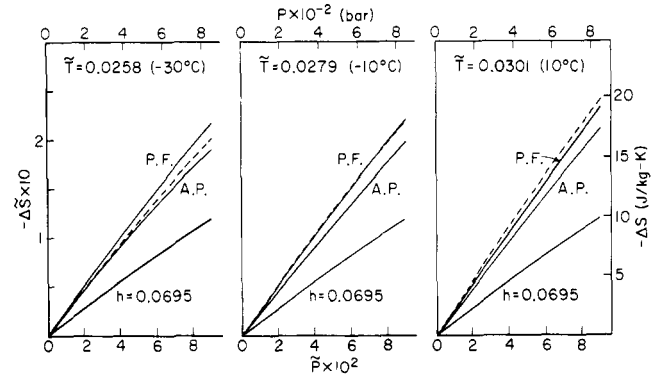

Figure 7. Compressional entropy as a function of pressure for high pressure glass ($\tilde{P}' = 0.0853$). Dashed lines, experimental (Tait equation); solid lines, A.P., P. F., and frozen parameter assumption.

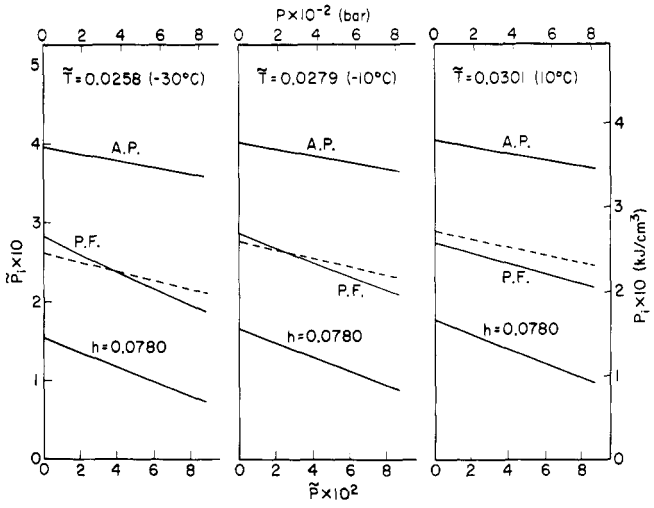

Figure 8. Internal pressure as a function of pressure at three temperatures for low pressure glass ($\tilde{P}' = 0$). Dashed lines, experimental, A.P. adjusted parameter, $h = 0.0780$ frozen parameter assumption.

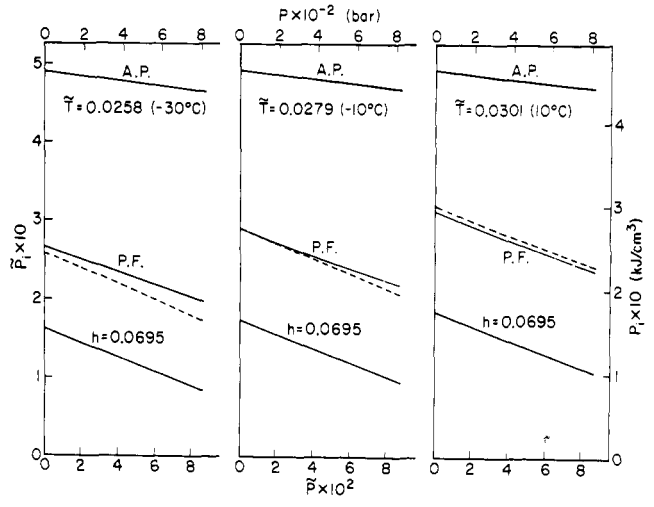

Figure 9. Internal pressure as a function of pressure at three temperatures for high pressure glass ($\tilde{P}' = 0.0853$). Designations as in Figure 8.

marked as A.P. in Figures 6 and 7 were obtained by means of eq 13 and serve as illustrations for the subsequent discussion.

A consistent procedure however requires the proper use of a configurational partition function to obtain, at this stage from experiment, the function $y(\tilde{T},\tilde{V})$. Retaining the formal expression for Z [eq 1–3, ref 7], the approach to be employed now is, accordingly, to solve the partial differential equation in y represented by the pressure relation [eq 6] for given experimental P, V, and T. $(\partial\tilde{F}/\partial y)_{\tilde{V},\tilde{T}}$ is given explicitly by eq 8 and the expression for $(\partial\tilde{F}/\partial\tilde{V})_{\tilde{T},y}$ [eq 9] is identical with that for $-\tilde{P}$ for the liquid state. A numerical iteration method similar to Newton's has been employed. The computation procedure is described in the Appendix and illustrated in Figure 14. The numerical solutions for $h = 1 - y$ can be expressed by biquadratic polynomials in $\tilde{T}$ and $\tilde{V}$ for which the coefficients and the residual standard deviations are given in Table Ia for the liquid and the two glasses. As with other polynomials given in this paper the coefficients have been determined by least-squares fits. Using the sequential "F" test,[9] the insignificant coefficients have been deleted, and the significant ones recalculated from the remaining variables. Table Ib gives h as a function of $\tilde{T}$ and $\tilde{P}$, which may be used to calculate the thermodynamic functions presented later in this paper. Note that the $\tilde{T} - \tilde{V}$ expressions are more accurate, in particular for the liquid state. In these representations only those for the liquid are universal. Since no theoretical constraint condition has been established for the glassy state, the others apply only to this polymer under these particular glass formation conditions. The liquid coefficients may be used to facilitate calculations of the pressure and thermodynamic functions in lieu of complicated iteration methods.

In Figure 3 are shown the curves P.F. (partition function) for the hole fraction $h = 1 - y$ obtained from the differential equation [eq 6] as a function of pressure at −30, −10, and 10 °C. They may be compared with the results (A.P.) obtained by considering the term P_1 solely in eq 6, i.e., eq 11. The differences are significant with the former being closer to the values at T_g. The two sets of h functions are however quite close, particularly at low pressures and elevated temperatures.

The resulting variations of energies and entropies with pressure relative to atmospheric pressure appear in Figures 4–7. In general a noteworthy improvement over the previous treatment is observed. The remaining deviations are small indeed. One reason for these are the numerical approximations in solving eq 6 for y with experimentally determined parameters. For analysis it is convenient to express both $\tilde{U}$ and $\tilde{S}$ in biquadratic form, which facilitates the calculation of certain second-order functions. The coefficients for $\tilde{U}(\tilde{T},\tilde{V})$ are given in Table IIa from which the internal pressure, $P_i = (\partial U/\partial V)_T$, and the configurational heat capacity $C_v = (\partial U/\partial T)_V$ are readily obtained. The corresponding coefficients for $\tilde{U}(\tilde{T},\tilde{P})$ are given in Table IIb along with those for $\tilde{S}(\tilde{T},\tilde{P})$, which may be used to calculate the configurational heat capacity $C_p = (\partial U/\partial T)_P$. Note that as with the h polynomials, the $\tilde{T} - \tilde{V}$ representation is more accurate as indicated by the residual standard deviations. Again, those for the liquid are universal, whereas those for the glasses are not.

We turn next to the internal pressure, P_i. With the liquid and adjustable parameter (A.P.) calculation for the glasses, the determination of P_i from the theoretical relationships is relatively simple. With the proper employment of the partition function (P.F.), however, it is far more convenient to obtain P_i from appropriate differentiation of the polynomial expressed in Table IIa. The computed (A.P. and P.F.) and the experimental results are presented in Figures 8 and 9. Here the adjustment procedure (curves labeled A.P.) yields large deviations of similar magnitude and opposite sign compared with the results for constant hole fraction h. Obviously the variation of y and $\tilde{T}$ and $\tilde{V}$ required to satisfy the experimental equation of state based on eq 11 is too large. A considerable improvement ensues from the reduction in this

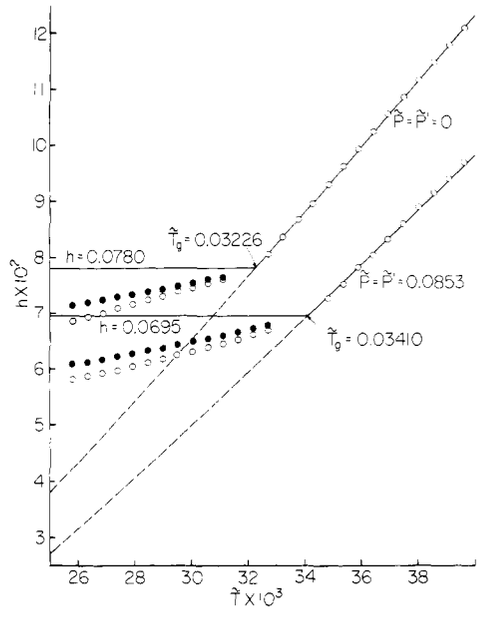

Figure 10. Comparison of hole fraction h as a function of temperature for two glasses with $P = P'$ and their equilibrium melts. Solid lines theoretical and "freeze-in" assumption, respectively. Dashed lines theoretical, undercooled melt. Open and closed circles, adjustable parameter and partition function procedure, respectively.

variation shown in Figure 3, when the partition function is employed in the proper manner as implied in the polynomial. The consequences of the numerical approximations are of course magnified in the derivatives. Since P_i is purely a compressional function and since we have no constraint equation for the glass, the differences between the experimental and theoretical (P.F.) values of P_i are artifacts introduced by the numerical analysis, involving the imprecision of the Tait equation and the numerical manipulation of the theoretical equation of state. This argument does not hold, however, in the liquid region, or with the thermal properties, for example, the configurational heat capacities, in both liquid and glass, as will be discussed.

C. Temperature Dependence of Thermodynamic Functions for the Liquid–Glass System. In order to study the behavior at the glass transition, it is useful to observe the temperature dependence of the thermodynamic functions over the liquid and glassy ranges together. In Figure 10 the hole fraction is plotted as a function of temperature for the liquid and two glasses at $P = P'$ for 0 and 800 bar. Note that the proper use of the partition function (designated P.F.) gives more constant response for the glasses than that obtained from the adjustable parameter (A.P.) calculations. Although the h–T curves appear to be essentially linear for the glasses (as indicated in Table Ib), slight, but significant, departures from linearity exist for the liquid over the range indicated.

From the coefficients in Table Ib the freezing fractions

$$F_T = 1 - \left[\left(\frac{\partial h}{\partial T}\right)_{P,\text{glass}} \Big/ \left(\frac{\partial h}{\partial T}\right)_{P,\text{liquid}} \right] \qquad (19)$$

and

$$F_P = 1 - \left[\left(\frac{\partial h}{\partial P}\right)_{T,\text{glass}} \Big/ \left(\frac{\partial h}{\partial P}\right)_{T,\text{liquid}} \right]$$

are readily determined. These fractions are bounded between 0 and 1 where the lower bound indicates no distinction between the h derivatives for liquid and glass, and the upper bound applies to constant h in the glass. The results are tabulated at selected conditions in Table III. The first two sets of conditions (T,P) are at the respective T_g's for the $P' = 0$ and 800 bar glasses. Since the T_g's are slightly out of range of the experimental data, the third set (0.02794, 0), which is about mid range for both data sets and hence more accurate, is included. The quantities are always evaluated at the same conditions for both glasses. From Table III and Figure 10 the following trends are apparent:

(1) The magnitudes of the h derivatives and freezing fractions when evaluated properly from the partition function are smaller and larger, respectively, than those using the adjustable parameter method. This means that the glass structure is more "frozen in" than indicated previously.[2] (2) F_P is usually larger than F_T (consistently larger for the P.F. calculations). No theoretical justification for this trend is apparent at this time. (3) There is essentially no difference between the respective freezing fractions for the two glasses when evaluated at the same conditions. This relationship holds for both A.P. and P.F. computations.

In some cases the values in Table III differ slightly from the corresponding ones in Table IV of paper I. These differences result from the different numerical procedures used in the evaluations. Also, it appears that the freezing fractions can

Table III
Hole Fraction Derivatives and Freezing Fractions

	Liquid, $\tilde{T}$, $\tilde{P}$					
	0.03226, 0		0.03410, 0.0853		0.02794, 0	
$(\partial h/\partial \tilde{T})_{\tilde{P}}$	5.70		4.79		5.52	
$-(\partial h/\partial \tilde{P})_{\tilde{T}}$	0.245		0.179		0.188	
	Glasses					
	A.P.	P.F.	A.P.	P.F.	A.P.	P.F.
$\tilde{P} = 0$	$\tilde{T} = \tilde{T}_g$					
$(\partial h/\partial \tilde{T})_{\tilde{P}}$	1.46	1.04	1.26	0.96	1.46	1.04
$-(\partial h/\partial \tilde{P})_{\tilde{T}}$	0.051	0.029	0.056	0.030	0.042	0.025
F_T	0.74	0.82	0.74	0.80	0.74	0.81
F_P	0.79	0.88	0.69	0.83	0.78	0.87
$\tilde{P}' = 0.0853$			$\tilde{T} = \tilde{T}_g$			
$(\partial h/\partial \tilde{T})_{\tilde{P}}$	1.42	1.07	1.26	0.95	1.42	1.07
$-(\partial h/\partial \tilde{P})_{\tilde{T}}$	0.044	0.027	0.048	0.030	0.036	0.021
F_T	0.75	0.81	0.74	0.80	0.74	0.81
F_P	0.82	0.89	0.73	0.83	0.81	0.89

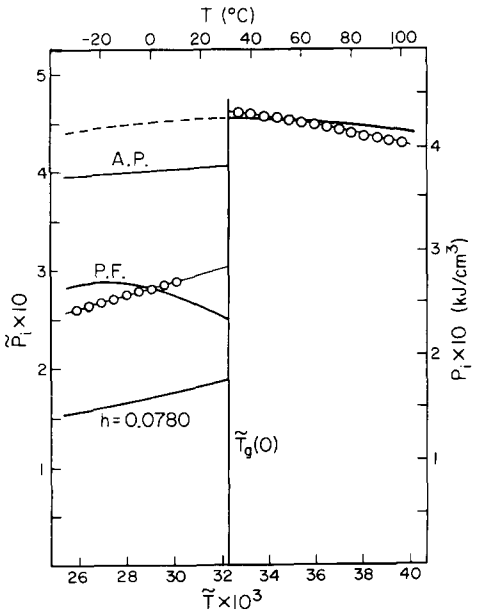

Figure 11. Internal pressure as a function of temperature at atmospheric pressure for low pressure glass ($\tilde{P}' = 0$) and equilibrium liquid. Circles, experimental; solid lines, theoretical. Designations for glass as in Figure 8.

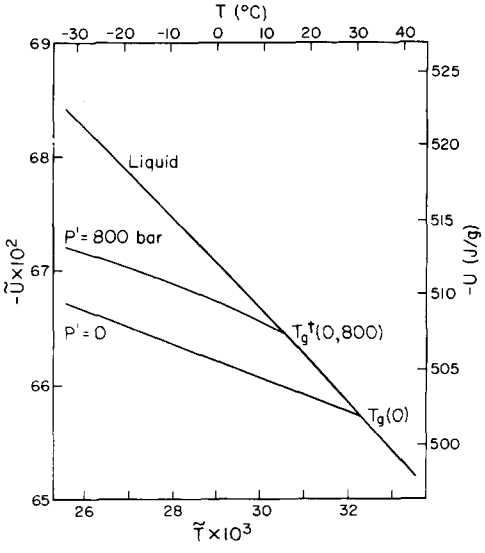

Figure 12. Comparison of internal energy as a function of temperature for undercooled melt (theory), low and high pressure glass, all at atmospheric pressure.

only be determined to within two significant figures as is indicated in Table III of this paper.

The temperature dependence of the internal pressure is illustrated in Figure 11 at atmospheric pressure for the $P' = 0$ glass. In particular, since the temperatures are extended into the liquid region, this presentation illustrates the difference between the liquid and glass at T_g. As mentioned earlier the differences between the experimental and theoretical internal pressures in the glass are artifacts resulting from inprecision of the numerical analysis used on both the experimental data and theoretical formulation. Accordingly, it is not clear whether the maximum in P_i is real in the glass, as revealed by the theoretical curve. Table IV summarizes the experimental and theoretical values at T_g. The former also include those estimated from Figure 2 of ref 10, which are in good agreement with ours, particularly in the liquid state. The data in ref 10

Table IV
Theoretical and Experimental Internal Pressures at T_g = 30.7 °C

	Experimental			
	Ref 2	Ref 10 Sample 1	Ref 10 Samples 2, 3, 4	Theoretical
$P_{i,l}$, kJ/cm³	0.434	0.427	0.439	0.425
$P_{i,g}$, kJ/cm³	0.282	0.259	0.272	0.232
ΔP_i, kJ/cm³	0.152	0.168	0.167	0.193
$\tilde{P}_{i,l}$, reduced	0.463	0.455	0.468	0.454
$\tilde{P}_{i,g}$, reduced	0.301	0.276	0.290	0.247
ΔP_i, reduced	0.162	0.179	0.178	0.207

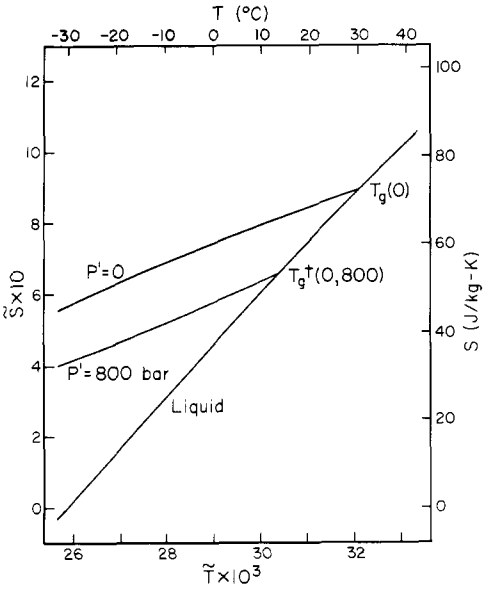

Figure 13. Comparison of entropy as a function of temperature for undercooled melt (theory), low and high pressure glass, all at atmospheric pressure. Value for liquid set equal to zero at −30 °C.

were actually taken at nearly constant volume conditions with a small correction applied to account for the response of the dilatometer. The agreement between the two sets of data confirms that $(\partial P/\partial T)_V$ does not necessarily have to be obtained at constant volume conditions even during glass formation, and that the Tait equation is sufficiently accurate for the evaluation of P_i.

We now examine some of the functions which cannot be determined from PVT data alone. As an illustration, the internal energies of the undercooled melt and of the two glasses, all at atmospheric pressure, are compared in Figure 12 with each other. For example, at −30 °C, i.e., about 60° below the normal glass temperature, the difference between the equilibrium liquid and the low pressure glass amounts to 12.6 J/g or 1.08 kJ/mol, if the molecular weight of the repeat unit is taken as 86.1 g/mol. This is reduced to 8.8 J/g in the depressurized high pressure glass, thus yielding a difference of 3.8 J/g between the two glasses. In Figure 13 the corresponding entropy diagram is displayed. We observe differences of 0.046 and 0.033 J/(gK) between liquid and the two glasses, with a corresponding reduction of the entropy by 0.013 J/(g K) due to densification. Note that in Figure 13 the entropies are defined relative to the equilibrium value at −30 °C, which is set equal to zero.

Finally we turn to a consideration of the specific heats C_p and C_v for which the theoretical and experimental values are

Table V
Theoretical and Experimental
Heat Capacities at T_g = 304 K

	Liquid		Glass (P' = 0)
Cp(theo)[a]	0.337		0.103
Cp(exptl)	1.77		1.27
Cp(theo)/Cp(exptl)	0.190		0.081
$Cp - C_v$(exptl)	0.250		0.055
$Cp - C_v$(exptl)	0.261		0.069
C_v(theo)	0.087		0.048
C_v(exptl)	1.51		1.20
C_v(theo)/C_v(exptl)	0.057		0.040
ΔCp(theo)		0.234	
ΔCp(exptl)		0.50	
ΔCp(theo)/ΔCp(exptl)		0.47	
ΔC_v(theo)		0.039	
ΔC_v(exptl)		0.31	
ΔC_v(theo)/ΔC_v(exptl)		0.13	

[a] C_p units in J/(g K).

summarized at T_g = 304 K in Table V. Since experimental data are usually available only at atmospheric pressure, we need to compute values at $P = P' = 0$ only. Of course we can discuss only the intermolecular contributions here. The theoretical values in Table V are obtained from the polynomial expressed in Tables IIa and IIb applying the definitions $C_p = T(\partial S/\partial T)_P$ and $C_v = (\partial U/\partial T)_V$. Using the scaling factor S^* = 0.08107 J/(g K), these quantities are evaluated at $\tilde{T}_g$ = 0.03226 (30.7 °C) at which $\tilde{V}$ = 1.0356 (0.8431 cm³/g). From the PVT data we obtain the difference

$$C_p - C_v = TV\alpha^2/\kappa \tag{20}$$

where α and κ are the thermal expansivity and isothermal compressibility, respectively. Equation 20 stipulates that the difference between total heat capacities (obtained from calorimetry) is purely configurational. From the theoretical values we obtain $C_p - C_v$ = 0.250 J/(g K) for the liquid and 0.055 for the glass. These values compare with the corresponding experimental ones, 0.261 and 0.069, respectively, which are derived by using $\alpha_l = 7.117 \times 10^{-4}$ K^{-1}, $\alpha_g = 2.795 \times 10^{-4}$ K^{-1}, $\kappa_l = 4.981 \times 10^{-5}$ bar^{-1}, and $\kappa_g = 2.896 \times 10^{-5}$ bar^{-1}, taken from Table 9(b) of ref 3. The amount of agreement, 4% for the liquid and 20% for the glass, reflects the validity of the liquid theory and the accuracy of the numerical analysis used here.

We will now compare the configurational heat capacities obtained from the theory with the total values derived from calorimetry and PVT measurements. Mr. James J. Weeks of the National Bureau of Standards has made C_p measurements on a specimen of our sample using DSC. The liquid and glass limiting values in J/(g K) near T_g may be represented by the linear equations

$$C_{p,l} = 1.135 + 0.00209T$$

$$C_{p,g} = 0.402 + 0.00284T$$

where the latter applies to the glass formed by cooling at 0.31 K/min. Since no significant difference in $C_{p,g}$ was observed between this rate and 2.5 K/min, we assume that there would be essentially no difference if the formation rate were 5 K/h as with the PVT data.[3] From the above equations the values at T_g = 304 K are $C_{p,l}$ = 1.77 and $C_{p,g}$ = 1.27 with the difference ΔC_p = 0.50 J/(g K). Thus the intermolecular contribution is about 19% obtained from the ratio of the theoretical and experimental values applicable to the liquid state. This may be compared with 12–13% for polystyrene and poly(methyl methacrylate), depending weakly on temperature. These values have been obtained by applying the scaling factors from ref 4a and 5, respectively, and taking the experimental data from ref 11. Note that the experimental value for ΔC_p (0.50) is comparable with the theoretical (configurational) value for the liquid (0.337) and considerably exceeds the computed ΔC_p = 0.234. Thus, according to this analysis the configurational contribution to the total ΔC_p is only 47%.

It is also of interest to determine the corresponding fraction for ΔC_v. Equation 20 is employed to determine the total value of C_v. Using the values of α and κ given above, we obtain $C_{v,l}$ = 1.51 J/(g K) and $C_{v,g}$ = 1.20, with the difference ΔC_v = 0.31. ΔC_v may be compared with ΔC_p with the fraction $\Delta C_v/\Delta C_p$ = 0.62. With the corresponding theoretical values tabulated above, the configurational contribution to the total ΔC_v is 13%, compared with 47% for the corresponding ΔC_p.

In order to compare the entropies we make an estimate of the experimental difference $S_g - S_l$ for a reference temperature of 0 °C. In the standard relation

$$S_i = \int C_{p,i}\, dT/T + K_i$$

we employ for $i = l$ and $i = g$ the linear expressions shown above. The difference between the integration constants $K_g - K_l$ is determined from the condition $S_g = S_l$ at $T = T_g$. Hence we have

$$\Delta S = S_g - S_l = -0.733 \ln T + 0.00075T + 3.963$$

For T = 273.15, the result is ΔS = 0.056 J/(g K). The relations shown in Table IIb yield at the same temperature $\tilde{S}_g - \tilde{S}_l = -4.937 + 5.223$, or ΔS = 0.0232 J/(g K), which indicates that about 42% of the change in entropy from liquid to glass is configurational.

Next it is of interest to separate the theoretical entropies for the undercooled melt and glass into a lattice and a hole contribution by writing

$$S_{hole} = S(y) - S(1)$$

where the last term corresponds to the simple cell model with the square well approximation for the cell potential.[7]

From eq 13 we have

$$\tilde{S}(1) = 3 \ln (\tilde{V}^{1/3} - 2^{-1/6}) + \ln V^* + \text{const} \tag{13'}$$

The experimental volumes for the two glasses and the computed volume for the undercooled liquid are to be substituted in eq 13′. The results at −30 and 0 °C are listed in Table VI. The differences in the configurational entropy $S(y)$ are those seen also in Figure 13 and amount to about 0.01 J/(g K) for the two glasses. They are due primarily to differences in the hole contribution. With increasing temperature this contribution increases, and is smaller for the undercooled melt, as is to be expected. The linearity of the plots in Figure 13 results in the expression for the configurational specific heat,

$$C_p = (\Delta S/\Delta T)T$$

and Table VI then yields for the ratio $\Delta S_{hole}/\Delta S = C_{p,hole}/C_p$ 0.62, 0.59, and 0.56 for liquid, low, and high pressure glass, respectively. For the glasses these results once more illustrate the significance of hole contributions, shown earlier in terms of the thermal expansion.

The above results imply that the entropy and heat capacities, and their changes at T_g, are dominated by contributions from vibrational modes. Before accepting the validity of this result, one should consider the possible existence of certain errors which could exaggerate the dominance of the role of the vibrational modes. On the experimental side, the linear extrapolation of $C_{p,l}$ to 0 °C in the computation of the entropy may be questioned. Actually an alternative value reviewed in the literature[12] is ΔC_p = 0.48 J/(g K), which would increase

Table VI
Entropies of Undercooled Melt and Glasses at Atmospheric Pressure[a]

	$\tilde{V}$	y	$-S(y)$ + const	$-S(1)$ + const	S_{hole}	$S_{hole}/(-S(y)$ + const)
		$\tilde{T}$ = 0.02581 (−30 °C)				
Liquid	0.9953	0.9578	0.4772	0.5590	0.0817	0.171
Glass (P' = 0)	1.0181	0.9285	0.4314	0.5425	0.1111	0.258
Glass (P' = 800 bar)	1.0110	0.9375	0.4442	0.5475	0.1033	0.233
		$\tilde{T}$ = 0.02900 (0 °C)				
Liquid	1.0147	0.9404	0.4401	0.5449	0.1049	0.238
Glass (P' = 0)	1.0266	0.9254	0.4172	0.5367	0.1195	0.286
Glass (P' 800 bar)	1.0194	0.9344	0.4309	0.5416	0.1107	0.257

[a] Entropy Units: J/(g K).

the ratio of the configurational to the total ΔC_p at T_g from 47 to 49%. By extrapolation of the data with temperature in ref 13 we obtain the value $\Delta C_p = 0.41$ at T_g, which would further increase this ratio to 57%. On the other hand, the value $\Delta C_p = 0.59$ obtained from the measurements of Angell and Tucker[14] on a specimen from our sample would decrease this ratio to 40%. The maximum difference between these values (40 to 57%) is a reflection of the uncertainty of C_p measurements on substances with identical polymeric repeat units. On the theoretical side a source of error in the computed value can be the numerical approximations in evaluating h from the experimental equation of state (see Appendix), since any errors are magnified in the required derivatives. Assuming the configurational contribution is too small, one may then invoke a particular inadequacy of the partition function in respect to the entropy quantities. Again Figures 2, 6, and 7 do not indicate such, at least as far as the pressure dependence is concerned. We are then led to a basic assumption made concerning the glassy state, namely that the only difference or connection between equilibrium melt and glass arises from the behavior of the structural parameter h. One may argue that an additional structural factor should be the number of external degrees of freedom $3c$ (or its variation with temperature) which is inversely related to the temperature scaling factor T^*. An abrupt change in T^* at T_g is not permitted because it would correspond to an actual temperature jump. However, a gradual increase in T^* with decreasing real temperature commencing at T_g is permissible. An effective increase in T^*, or reduction in $\tilde{T}$, for a given reference temperature T below T_g, would produce a smaller configurational heat capacity in the glass, which would correspond to a larger configurational difference at T_g. This result would also express a change in the vibrational contribution to the heat capacity in the T_g process. This is an example of how a portion of the vibrational modes may depend on the configurational state.

Concluding Remarks

We have arrived at a consistent description of the temperature and pressure dependent thermodynamic properties of constant formation glasses. This is obtained in terms of a partition function of the identical form as for the equilibrium system, but with the expressions generalized to include nonequilibrium conditions, and with the h function evaluated from the experimental PVT surfaces. In paper I h was treated as an adjustable parameter obtained from the pressure equation strictly applicable to equilibrium, or alternatively, to constant h conditions, neither of which are satisfied for these glasses. There also h was evaluated from the experimental PVT surface. Aside from the element of consistency, the quantitative agreement of the computed thermodynamic functions with experiment is significantly enhanced, particularly for the internal pressure. On the other hand, it is gratifying to observe the good estimate of ΔU and ΔS which is derived from the much simpler adjustable parameter method. This results from the fact that h and the ensuing freezing fractions F_T and F_P are not very different between the two procedures. Thus it appears that the simplified procedure is quantitatively almost as adequate, except in respect to the internal pressure.

In paper I we suggested that the same values of the freezing fraction F_T for the low (P' = 0) and high (P' = 800 bar) pressure glasses might be consistent with a unique entropy surface with respect to varying formation pressure. This notion is, of course, inconsistent with the results of our analysis for which the discrete entropy functions are displayed in Figure 13.

The concept of a single entropy surface originates from the apparent general validity of the equation

$$dT_g/dP = TV\Delta\alpha/\Delta C_p \tag{21}$$

as pointed out by O'Reilly[15] from experimental data on different glass-forming substances. From simple phenomenology Goldstein[16] has shown that eq 21 implies a single entropy surface with respect to formation pressure. On the other hand, it is clear from overwhelming PVT data that the corresponding volume is not unique, a result which is consistent with the experimentally determined inequality

$$dT_g/dP < \Delta\kappa/\Delta\alpha \tag{22}$$

Since we are employing equations of state of the form $V = V(T,P,h)$ and $S = S(T,P,h)$, it is clear that the hole theory as applied here cannot explain the coexistence of a single entropy and manifold volume surfaces. This statement has already been implied in our earlier comments on heat capacity.

Incidentally, this result is consistent with that implied from the orderng parameter analyses presented in ref 17–20. When only one ordering parameter is considered, eq 21 and the equation corresponding to (22) are satisfied. Since both of these relations are now equations, they imply that both the volume and entropy surfaces are unique.[16] We cannot, however, apply this result as obtained from the works referenced above because in all of these the ordering parameters are taken to be frozen in the glass, whereas, in our case, h varies in the glass.

At this juncture it is pertinent to refer to calorimetric data on densified polymeric glasses of styrene and methyl methacrylate.[21,22] Within experimental error, the enthalpy of the densified polymer appears to be indistinguishable from that of the "normal" one up to formation pressures of 800 bar. Thereafter, and up to their maximum value (2600 bar), a significant rise of the enthalpy difference $H(0,P') - H(0,0)$ [where $H = H(P,P')$ is taken isothermally] is observed. The densified polymer having the larger enthalpy is contrary to our theoretical predictions as seen in Figure 12 (recalling that U and H are indistinguishable at atmospheric pressure).

However, again we note the consistency in respect to the function ΔU for both glasses (see Figures 4 and 5), with the derivation of the h function from the PVT surfaces. To account formally for the interchange of the two glass surfaces shown in Figure 12, one could allow a variation of T^* as suggested in the last section. If then T^* (pressurized glass) < T^* ("normal" glass), this would increase the energy of the pressurized glass (relative to the "normal" one) with a corresponding increase in T_g† applicable to the energy or enthalpy. The above inequality results in the opposite one for c, the number of external degrees of freedom. Thus the pressurization process during glass formation could be assumed to enhance the importance of the external relative to internal modes, or to reduce the freeze-in process.

As indicated by this and earlier work, the liquid state theory is adequate to describe the PVT behavior of polymers in general. We still need a satisfactory *theoretical* constraint condition to apply to the glasses. Also, we would like to predict the location of T_g. Since it has been observed on the polymers so far evaluated[8] that $0.018 \leq \tilde{T}_g \leq 0.036$, $\tilde{T}_g$ can hardly be considered to be a corresponding temperature. This precludes the possibility of predicting the value of T_g for each polymer from its scaling factor T^*.

We have considered for the first time explicitly intermolecular contributions to the heat capacities. Since we do not have corresponding experimental data on configurational heat capacities, we do not know if the ratios (configurational to total) given in this paper are reasonable; however, it is possible that there are other ways to estimate these fractions. In order to obtain a better understanding of the thermal behavior, a more detailed study of specific heats encompassing a variety of polymeric structures in a manner analogous to our earlier PVT investigations is called for.

Note Added in Proof: Since preparation of this manuscript, Sasabe and Moynihan [23] have measured C_p on a specimen of our sample of PVAC. At T_g = 304 K their values of C_p for both liquid and glass exceed ours (Table V) by 0.06 J/(g K) with values of ΔC_p being identical. Application of their results to our analysis would not alter the conclusions given in this paper.

Acknowledgment. The authors are indebted to Dr. Charles M. Guttman for his assistance and suggestions on preparation of this manuscript and to Mr. James J. Weeks for obtaining heat capacity data on our sample of PVAc. This work was supported in part by the National Science Foundation under Grants GH-36124 and DMR 75-15401 to Case Western Reserve University.

Appendix

It is desired to obtain numerical solutions of the isothermal differential equation

$$-\tilde{P} = f_1(\tilde{T},\tilde{V},y) + f_2(\tilde{T},\tilde{V},y)(\partial y/\partial \tilde{V})_{\tilde{T}}$$

where $f_1 = (\partial \tilde{F}/\partial \tilde{V})_{\tilde{T},y}$ is equal to $-\tilde{P}$ for the equilibrium state [see eq 7 in ref 7] and $f_2 = (\partial \tilde{F}/\partial y)_{\tilde{T},\tilde{V}}$. Accordingly the explicit dependencies of these functions on their arguments are:

$$f_1 = -(\tilde{T}/\tilde{V})[1 - 2^{-1/6}y(y\tilde{V})^{-1/3}]^{-1} - (2y/\tilde{V})(y\tilde{V})^{-2} \times [1.011(y\tilde{V})^{-2} - 1.2045] \quad \text{(A1)}$$

$$f_2 = -(3\tilde{T}/y)[1 + \ln(1-y)/y] + (3\tilde{T}/y)[2^{-1/6}y(y\tilde{V})^{-1/3} - \tfrac{1}{3}][1 - 2^{-1/6}y(y\tilde{V})^{-1/3}]^{-1} + \tfrac{1}{2}(y\tilde{V})^{-2}[2.409 - 3.003(y\tilde{V})^{-2}]$$

In solving eq A1 iterations were used where the new ith derivative was approximated successively by

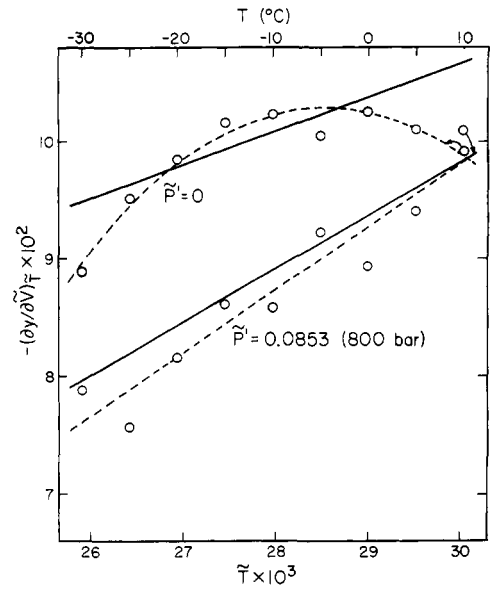

Figure 14. $(\partial y/\partial \tilde{V})_{\tilde{T}}$ vs. reduced temperature for constant formation glasses. Open circles, secant values obtained from eq A1 and A2. Dashed lines, regressions on open circles, quadratic for $\tilde{P}' = 0$, linear for $\tilde{P}' = 0.0853$. Solid lines, values obtained from differentiation of eq 10 applicable to all data points.

$$(\mathrm{d}y/\mathrm{d}\tilde{V})_{\mathrm{new},i} = \{[y(\tilde{P}_1) - y(0)]/[\tilde{V}(\tilde{P}_1) - \tilde{V}(0)]\}_{\mathrm{new},i} \quad \text{(A2)}$$

for which the iteration process

$$(dy/d\tilde{V})_{\mathrm{old},i+1} = [(dy/\mathrm{d}\tilde{V})_{\mathrm{old},i} + (\mathrm{d}y/\mathrm{d}\tilde{V})_{\mathrm{new},i}]/2$$

was found to converge in all cases. That is, the difference between the old and new derivatives became insignificant after about six iterations with the initial (i = 1) old value of $(\partial y/\partial \tilde{V})_{\tilde{T}}$ set equal to zero. In this work the value of $\tilde{P}_1$ was taken to correspond to the highest experimental pressure, 800 bar.

The above procedure yields one value of $(\partial y/\partial \tilde{V})_{\tilde{T}}$ for each temperature from the data at P = 0 and 800 bar. These results are illustrated by the circles in Figure 14. The dashed lines are their regressions (quadratic for $\tilde{P}' = 0$ and linear for $\tilde{P}' = 0.0853$) with respect to temperature.

As $T \to T_g$, $f_2 \to 0$ (corresponding to the equilibrium minimization condition) and the differential equation degenerates into an algebraic one, i.e., $-\tilde{P} = f_1$. This has the consequence that the fraction on the right-hand side of

$$(\partial y/\partial \tilde{V})_{\tilde{T}} = -(\tilde{P} + f_1)/f_2$$

takes the form 0/0 as $T \to T_g$. The limit of this ratio is, however, a determined quantity. This forces $(\partial y/\partial \tilde{V})_{\tilde{T}}$, and thus $(\partial y/\partial \tilde{T})_P$ illustrated in Figure 10, to be unique as $T \to \tilde{T}_g$. This condition represents the seemingly missing boundary condition for the partial differential equation.

From the above procedures a set of y values is derived as a function of temperature and volume for which $(\partial y/\partial \tilde{V})_{\tilde{T}}$ and $(\partial y/\partial \tilde{T})_{\tilde{V}}$ may be evaluated. However, the values of $(\partial y/\partial \tilde{V})_{\tilde{T}}$ are only secant values obtained from $y(\tilde{V})$ at 0 and 800 bars. In order to test the procedure and utilize the results at all data points for the two constant formation glasses, the values of $(\partial y/\partial \tilde{V})_{\tilde{T}}$ obtained from the regression equation (depicted by dashed lines in Figure 14) were then applied to eq 6. The new values of y were then fitted to polynomials in $\tilde{T}$ and $\tilde{V}$ for which the results are included in Table Ia with $h = 1 - y$. The corresponding values of $(\partial y/\partial \tilde{V})_{\tilde{T}}$ are illustrated by the solid lines of Figure 14, which, for our purposes, are considered to be in agreement with the dashed lines. Note that for $\tilde{P}' = 0$ only a linear temperature dependence is significant using data

points, in contrast to the quadratic dependence for the secant values. Now using Table Ia to redetermine $(\partial y/\partial \tilde{V})_{\tilde{T}}$ and then applying this result to eq 6 gives reasonably good agreement between the values of the new and old derivatives at each point, which is the final test for this procedure. The values of $(\partial y/\partial \tilde{T})_{\tilde{V}}$ also derived from Table Ia were used to evaluate the entropy from eq 7. Using this method, $(\partial y/\partial \tilde{V})_{\tilde{T}}$ and $(\partial y/\partial \tilde{T})_{\tilde{V}}$ are compatible in the sense that they correspond to the same solution.

References and Notes

(1) (a) National Bureau of Standards; (b) Case Western Reserve University.
(2) J. E. McKinney and R. Simha, *Macromolecules*, **7**, 894 (1974).
(3) J. E. McKinney and M. Goldstein, *J. Res. Natl. Bur. Stand., Sect. A*, **78**, 331 (1974).
(4) (a) A. Quach and R. Simha, *J. Appl. Phys.*, **42**, 4592 (1971); (b) A. Quach, P. S. Wilson, and R. Simha, *J. Macromol. Sci., Phys.*, **9** (3), 533 (1974).
(5) O. Olabisi and R. Simha, *Macromolecules*, **8**, 211 (1975).
(6) A. Quach and R. Simha, *J. Phys. Chem.*, **76**, 416 (1972).
(7) R. Simha and T. Somcynsky, *Macromolecules*, **2**, 342 (1969).
(8) R. Simha and P. S. Wilson, *Macromolecules*, **6**, 908 (1973).
(9) N. R. Draper and H. Smith, "Applied Regression Analysis", Wiley, New York, N.Y. 1966, p 71.
(10) G. Allen, D. Sims, and G. J. Wilson, *Polymer*, **2**, 375 (1961).
(11) V. Bares and B. Wunderlich, *J. Polym. Sci., Polym. Phys. Ed.*, **11**, 861 (1973).
(12) R. F. Boyer, *J. Macromol. Sci., Phys.*, **7** (3), 487 (1973).
(13) M. V. Vol'kenshtein, "Structure of Glass", Vol. 2, Consultants Bureau, New York, N.Y., 1961, p 111 (translation).
(14) C. A. Angell, private communication.
(15) J. M. O'Reilly, *J. Polym. Sci.*, **57**, 429 (1962).
(16) M. Goldstein, *J. Phys. Chem.*, **77**, 667 (1973).
(17) R. O. Davies and G. O. Jones, *Adv. Phys.*, **2**, 370 (1953).
(18) E. A. DiMarzio, *J. Appl. Phys.*, **45**, 4143 (1974).
(19) M. Goldstein, *J. Appl. Phys.*, **46**, 4153 (1975).
(20) G. Rehage and W. Borchard, "The Physics of Glassy Polymers", R. N. Haward, Ed., Wiley, New York, N.Y., 1973, p 74.
(21) C. Price, R. C. Williams, and R. C. Ayerst, "Amorphous Materials", R. W. Douglas and B. Ellis, Ed., Wiley-Interscience, New York, N.Y., 1972, p 107.
(22) C. Price, *Polymer*, **16**, 585 (1974).
(23) Submitted to *Rep. Prog. Polym. Phys. Jpn.*

Intrinsic Viscosity of Polymers in Good Solvents

Petr Munk* and Michael E. Halbrook

Department of Chemistry, The University of Texas at Austin, Austin, Texas 78712.

Received July 7, 1975

ABSTRACT: A semiempirical interpretation of the Mark–Houwink relation $[\eta] = KM^a$ is proposed, which enables one to calculate easily the unperturbed dimensions of the polymer coil from the parameters a and K. It is postulated that there is no thermodynamic interaction among macromolecular segments within a short section of a chain with a characteristic number of segments N_0, estimated as $N_0 \sim 9$. This postulate enables one to calculate the unperturbed parameter K_θ. A test of the method on an extensive range of data for solutions of polystyrene and poly(methyl methacrylate) yields satisfactory results. The method is also applicable to nonvinyl polymers with rather different structures, e.g., polysiloxanes, polycarbonates, and cellulose derivatives.

In most theories of polymer solutions a linear macromolecule is modeled as a string of segments suspended in a solvent. The segments are connected by universal joints. The model is fully described by four parameters: (1) the number of segments, N; (2) the length of a segment, A; (3) the friction coefficient of a segment, ζ; and (4) a thermodynamic parameter expressed as the Flory–Huggins interaction parameter χ or the familiar Flory's expression $\psi(1 - \theta/T)$ or the binary cluster integral (the excluded volume of a segment) β.

All the characteristic quantities of a macromolecular solution (size of the macromolecular coil, relative viscosity, friction coefficient of a coil, virial coefficients, etc.) are then unique functions of these four parameters and of the number of macromolecules in a volume unit, n. Usually, the concentration is expressed in units of mass per volume, c, which is related to n as $c = nM/N_A$, where M is molecular weight and N_A is Avogadro's number. Note that the molecular weight is *not* a basic parameter of the theory of polymer solutions as it enters only as a result of our preference for concentrations expressed as c. Other parameters (molar volume of solvent, V_0; specific volume of macromolecules, $\bar{v}$) enter the theory in a similar way.

One of the five basic parameters, the friction coefficient ζ, influences only the hydrodynamic properties. Moreover, experimental evidence shows that for macromolecules with a sufficient degree of coiling (i.e., for a high enough number of segments, typically M larger than 10^4) the value of ζ is such that the coil is hydrodynamically in the limiting nondraining state. In this state, the hydrodynamic properties no longer depend on ζ and the number of basic parameters is reduced to four.

Most theories (see Yamakawa[1]), even when one is studying the dependence of various phenomena on the molecular weight of the macromolecule, assume that the number of segments N is always so large as to be effectively infinite when compared to small integers. Using this implicit assumption, one finds that the basic parameters are always combined into two parameters and that the properties of macromolecular solutions are fully described by the two-parameter theories. (Actually M and c are also used, but are not counted as parameters.) The two parameters are the unperturbed dimensions of a coil $\bar{r}_0^2/M$ and a parameter z, defined as:

$$z = BM^{1/2} \tag{1}$$

$$B = 2(3/2\pi)^{3/2}(\bar{v}^2/N_A V_0)(\bar{r}_0^2/M)^{-3/2}\psi(1 - \theta/T) \tag{2}$$

where $\bar{r}_0^2$ is the mean end-to-end distance of an unperturbed coil, i.e., the distance which exists if the parameter $\psi(1 - \theta/T)$ is zero and all other parameters are the same.

In the following we will restrict our attention to intrinsic viscosity $[\eta]$. The two-parameter theory predicts for $[\eta]$

$$[\eta] = K_\theta M^{1/2}\alpha_\eta^3 \tag{3}$$

$$K_\theta = \phi_0(\bar{r}_0^2/M)^{3/2} \tag{4}$$

$$\alpha_\eta^3 = 1 + bz + \ldots \tag{5}$$

The expansion factor for viscosity α_η^3 may be expanded by a McLaurin series, eq 5; the perturbation theory[2] yields b =